Turkish Journal of Electrical Engineering & Computer Sciences

http://journals.tubitak.gov.tr/elektrik/

Research Article

Turk J Elec Eng & Comp Sci
(2016) 24: 4995 – 5010

doi:10.3906/elk-1407-182

Power quality assessment in different wind power plant models

Hamid SHARIATPANAH*, Morteza SABOURI KENARI, Roohollah FADAEINEDJAD
Department of Electrical and Computer Engineering, Graduate University of Advanced Technology, Kerman, Iran

Received: 01.08.2014 • **Accepted/Published Online:** 15.10.2015 • **Final Version:** 06.12.2016

Abstract: In order to fully study the power quality of a grid-connected wind farm, a suitable model providing accurate output for wind farms is necessary. In this paper, different methods, which have been proposed in previous studies, are investigated with regard to the power quality problem using a squirrel-cage induction generator wind turbine. These models are different in terms of accuracy and simulation time. The question is: which method is more suitable for simulation of a wind farm? To answer this question, a criterion should be introduced to compare different modeling methods. Full turbine representation is introduced as the best criterion to compare equivalent models of a wind farm such as quasi-multiturbine representation, single turbine representation, and multiturbine representation. A typical medium-sized wind farm is simulated using the full model and several equivalent models. These equivalent models are compared with the full model considering the accuracy and simulation time (computational load). These models are used to calculate the voltage, flicker, active, and reactive powers at the point of common coupling. The TurbSim and RPM-Sim programs are used to simulate the wind profile and wind farm. Results show significant differences between equivalent models outputs.

Key words: Wind farm modeling, power quality, full turbine representation model, equivalent models, RPM-Sim, TurbSim

1. Introduction

In developed countries, wind energy is considered an important renewable energy source. It is predicted that 20% of total global energy will be supplied from wind energy by 2030 [1]. The growth of energy generation by wind power leads to an increase in the numbers and sizes of wind farms. Consequently, the number of turbines within a wind farm can be more than 200 [2]. Due to rapid growth and increasing penetration of wind farms in power systems, appropriate wind farm modeling is essential to predict wind farm behavior.

Historically, research on wind farms flourished in the last decade of the 20th century and became a hot scientific topic in the wind energy systems field in the first decade of the 21st century. Authors proposed some equivalent models (including probabilistic [3,4] and dynamic models) because modeling of wind farms including all wind turbines (WTs) increases the computational load. To investigate the power quality problem, a dynamic model is necessary. Many papers have been written about the various modeling methods of wind farms and dynamic modeling of the wind farm is the most common. Due to field studies, the dynamic modeling of wind farms has been proposed in various equivalent methods, which are different in terms of accuracy and simulation time. In [5], complete wind farm electromagnetic transient models were simulated for grid integration studies. The equivalent modeling with single turbine representation (STR) and some improvements on this method

*Correspondence: hamid.sh.panah@gmail.com

were presented in [2,6–9]. The equivalent modeling with multiturbine representation (MTR), and also different criteria for the grouping of the turbines, were presented in [2,6,10–12]. Wind farm modeling by using quasi-multiturbine representation (QMTR) was presented in [9,13] to study the impact of the wind power plant on the network's power quality. In this research, the abovementioned methods are compared with the full dynamic model of a typical medium-sized wind farm as a benchmark.

The main contribution of the paper is to establish a comprehensive comparison between different wind farm models studying different power quality issues (e.g., flicker, voltage, and power variations) with computational load considerations, using full turbine representation (FTR) that has not been considered before. The full dynamic model of the wind farm is the best criterion to compare different equivalent models but there are few papers that present the full model for wind farms. For example, a wind farm with 15 WTs was simulated in [6], whereas the implementation of the full dynamic model for large wind farms is considered difficult and even impossible [2,10], because of the vast computational effort and long simulation time.

In this research, new software packages (including TurbSim and RPM-Sim) are used to model a relatively large wind farm. The performance of the QMTR method, introduced in previous research [9,13], is evaluated and validated by comparing the QMTR with the FTR method. The results show the importance of modeling methods in wind farm studies. In this paper a full model is simulated for a medium-sized wind farm consisting of 39 fixed-speed WT (FSWT) units.

These models are used to calculate the voltage, flicker, active, and reactive powers in different equivalent models at the point of common coupling (PCC) bus. Results obtained from the STR, MTR, and QMTR models are compared with the full dynamic model. Differences between the full model and the equivalent models can be a criterion to measure the accuracy of the equivalent models. The equivalent models can be evaluated better if the computational load of the models is considered. Finally, the best model will be introduced considering the accuracy in comparison with FTR and its computational load.

There are various software packages to simulate WTs and wind farms. In this paper, VisSim software is used to model the wind farm [14]. This software has a toolbox called RPM-Sim that is used to study hybrid networks [15]. The WT model, taken from the toolbox, is used in this research. TurbSim is also used to simulate the wind input profile. Simulation results obtained from the model are used to observe the power and voltage variations at the PCC of the wind farm. These signals can be used to study power quality parameters.

2. Wind turbine model

It is important to have a good model for a WT as the main part of a wind farm. The modeling of the WT is explained in this section. There are the various types of WTs that can be utilized in a wind farm. In this research, it is assumed that the wind farm consists of FSWTs. In this type of WT, a squirrel-cage induction generator (SCIG) is connected to the WT shaft through a gearbox. As shown in Figure 1, the model of the FSWT consists of different parts, including the WT, drive train, generator, and grid connection. The modeling of these parts is explained in the following sections.

2.1. WT rotor model

The aerodynamic aspect of the WT is modeled as a WT rotor model. In this part, the aerodynamic torque is calculated using the following equation:

$$T_{\omega t} = \frac{P_{wind}}{\omega_{r-l}}, \tag{1}$$

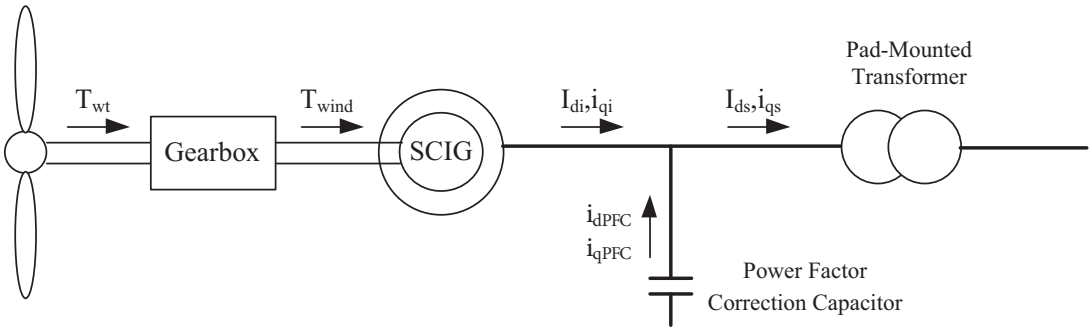

Figure 1. Configuration of fixed-speed induction machine.

where P_{wind} is the extracted power from the wind. It is calculated using the following equation:

$$P_{wind} = 0.5\rho\pi R_{bld}^2 C_p(\lambda,\theta)V_{wind}^3. \tag{2}$$

In this work, a stall-controlled WT is modeled. The nonlinear relation between tip speed ratio (TSR), λ, and C_p is encapsulated in the map block, which performs piecewise linear interpolated look-ups [16]. The TSR is calculated using the following equation:

$$TSR = \frac{\omega_{r-l}R_{bld}}{V_{wind}}, \tag{3}$$

where ω_{r-l} is the angular velocity of the blade that is obtained by Eq. (4):

$$\omega_{r-l} = \frac{\omega_r}{Gear_r} = \frac{0.1047.rpm}{Gear_r}. \tag{4}$$

The aerodynamic torque extracted from wind is considered as an input for the drive train model.

2.2. Drive train model

The aerodynamic torque is applied to the SCIG through the drive train. The drive train is modeled using various approaches such as one mass [17], 2 masses [6,7], and 3 or 6 masses models [18]. In this work, the one-mass model is used for the drive train model, high-speed and low-speed shaft, and gearbox that are considered as an equivalent mass, and the system dynamic is modeled using the following equations:

$$2H\frac{ds}{dt} = T_e - T_{wind}, \tag{5}$$

$$T_{wind} = \frac{T_{wt}}{Gear_r}. \tag{6}$$

2.3. Generation system

The generator dynamics are explained in this section. They are presented in the d-q frame as follows:

$$\psi_{ds} = \omega_b \int [v_{ds} - \frac{\omega}{\omega_b}\psi_{qs} + \frac{r_s}{X_{ls}}(\psi_{md} - \psi_{ds})dt, \tag{7}$$

$$\psi_{qs} = \omega_b \int [v_{qs} - \frac{\omega}{\omega_b}\psi_{ds} + \frac{r_s}{X_{ls}}(\psi_{mq} - \psi_{qs})dt, \tag{8}$$

$$\psi'_{dr} = \omega_b \int [v'_{dr} - \frac{\omega - \omega_r}{\omega_b}\psi'_{qr} + \frac{r'_r}{X'_{lr}}(\psi_{md} - \psi'_{dr})dt, \tag{9}$$

$$\psi'_{qr} = \omega_b \int [v'_{qr} - \frac{\omega - \omega_r}{\omega_b}\psi'_{qr} + \frac{r'_r}{X'_{lr}}(\psi_{mq} - \psi'_{qr})dt, \tag{10}$$

$$\psi_{md} = a\psi'_{dr} + b\psi_{ds}, \tag{11}$$

$$\psi_{mq} = a\psi'_{qr} + b\psi_{qs}, \tag{12}$$

where $a^{-1} = 1 + \frac{X'_{lr}}{X_m + X'_{ls}}$, $b^{-1} = 1 + \frac{X'_{ls}}{X_m + X'_{lr}}$. The constitutive flux linkage-currents are defined by the following equations:

$$\psi_{ds} = -L_{ss} i_{ds} + L_m I_{dr}, \tag{13}$$

$$\psi_{qs} = -L_{ss} i_{qs} + L_m I_{qr}, \tag{14}$$

$$\psi_{dr} = -L_{rr} i_{dr} + L_m I_{ds}, \tag{15}$$

$$\psi_{qr} = -L_{rr} i_{qr} + L_m I_{qs}. \tag{16}$$

It is important to note that rotor voltages v'_{dr} and v'_{dr} are considered zero for the SCIG. The induction generator output currents, i_{di} and i_{qi}, and electromagnetic torque T_e are defined using the following equations:

$$i_{qi} = f(\psi_{qs} - \psi_{mq}), \tag{17}$$

$$i_{di} = f(\psi_{ds} - \psi_{md}), \tag{18}$$

$$T_e = \frac{3P}{4\omega_b}(\psi_{ds} i_{qi} - \psi_{qs} i_{di}), \tag{19}$$

where $f^{-1} = X_{ls}$ and P is the generator poles. Eventually, to calculate the active power P_{IG}, the reactive power Q_{IG}, and the apparent power S_{IG} of the induction generator, the following equations are used.

$$P_{IG} = 3 \times 10^{-3}(v_{qs2} i_{qi} + v_{ds2} i_{di}) \tag{20}$$

$$Q_{IG} = 3 \times 10^{-3}(v_{qs2} i_{di} + v_{ds2} i_{qi}) \tag{21}$$

$$S_{IG} = 3 \times 10^{-3} \sqrt{v_{qs2}^2 + v_{ds2}^2} \sqrt{i_{qi}^2 + i_{di}^2} \tag{22}$$

3. System configuration

A typical wind power system, taken from [12], is studied in this research. The system configuration is shown in Figure 2. It shows a wind farm that consists of 39 identical FSWT units, each rated at 1 MW and 570 V. The WT generators (WTGs) are arranged on 9 daisy-chain branches. Each WTG unit is electrically attached to a transformer that steps up the voltage to a medium voltage level rated at 34.5 kV. A power factor correction capacitor, rated at 100 Mvar, is attached to each WTG. The typical values of the underground cable and overhead line impedance in Ω and per-unit (pu) can be found in [12]. Underground cable impedances between the 2 WTs are assumed constant but overhead line impedances between daisy-chain branches are different. The short-circuit level (SCL) and grid X/R ratio of this system are considered 100 MVA and 10.

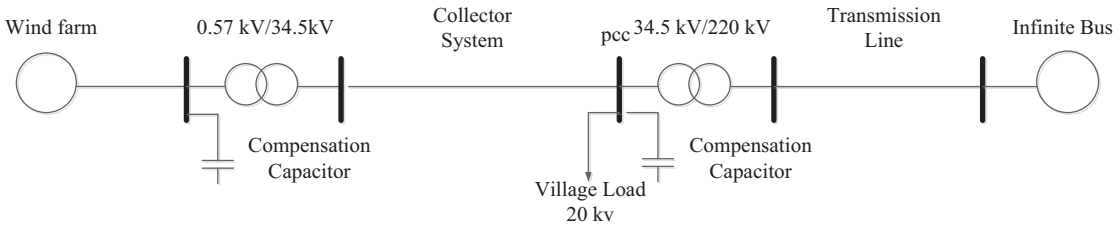

Figure 2. The single-line diagram of the typical wind farm connected to the grid.

Figure 3 shows a simplified single-line diagram of the wind farm connected to a substation. At the 34.5 kV level, the WTG units are connected to each other in a string or daisy-chain configuration, which is called the collector system. A village load of 20 kW and a compensation capacitor of 3300 kvar are connected to the PCC bus. The collector system is connected to a transmission system through the wind farm subtransmission transformer, which steps up the voltage to 220 kV at the PCC. The transmission system, consisting of lines rated at 220 kV, transfers the generated power to the power system, which is represented by an infinite bus.

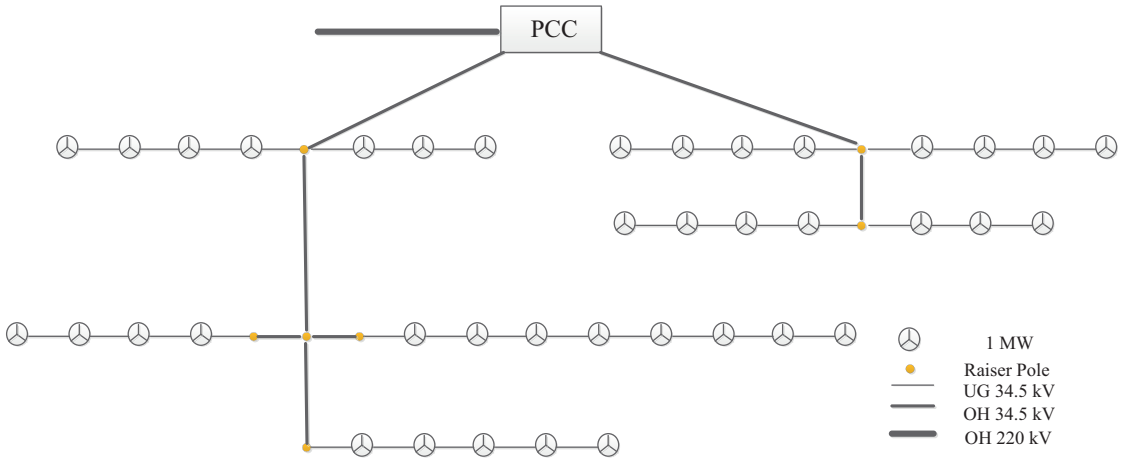

Figure 3. The wind turbine arrangement in a typical wind farm.

4. Wind farm model description

4.1. Equivalents and full turbine representation

The STR, MTR, QMTR, and FTR model are described below.

4.1.1. Single turbine representation (STR)

In this method, the WTG units can be replaced by an equivalent WTG unit rated at 39 $\times$ 1 MW. This work is applicable based on some network theory concepts, i.e. superposition effects. The electrical connections between the WTs within the wind farm are modeled by the collector system. The collector system can be represented by equivalent impedance as described in [11,19]. To simplify, the system can be considered as an integrated circuit with linear and resistor-inductor-capacitor (RLC) components.

The modeling of the wind farm with a WT and a wind input (STR model) is the worst-case assumption with regard to the power quality and transient stability issues. STR does not consider the complex behavior of the wind farm, since it does not consider the differences between input winds of each WT. It assumes that all of the WTs are synchronized; thus, the power quality at the PCC will be influenced by the same wind fluctuations, wind shear, and tower shadow effects.

4.1.2. Multiple turbine representation (MTR)

Wind farm modeling using several turbines is called MTR. In this method, each turbine can represent a group of WTs within the wind farm. This wind farm model would be appropriate when the collective behavior of all the turbines within the wind farm is considered. To achieve this goal, several WTs can be used to model different conditions. For example, the wind speed is different in various places of the wind farm. Each group of the WTs is modeled with one turbine and the same wind speed is considered for each group. MTR is a more realistic model rather than the STR, because the diversity of the WTs and aggregate impact are included in this model [2].

There are various criteria for the grouping of the WTs within a wind farm. Some important criteria are:

- Wind speed: Wind speed is one of the most important criteria for the WT grouping. The wind speed in various parts of the wind farm is more divergent with expansion and increasing of the area of the wind farm. Similarly, altitude and diversity may be found in a large wind farm, which will lead to differences in wind speeds experienced by each WT [12]. The MTR method is implemented according to the wind speed criterion explained in [6,8,11,18].

- WT type: Several types of WTs can be used in the wind farm. The expansion of the wind farms and improvement in the construction of new turbines over several years cause diversity in WT types within a wind farm. The diversity includes the size, the model, the production data, and the manufacturer [2]. The MTR method can be performed based on the WT type criterion [2,7,10].

- Control strategies: WTs can have various control algorithms. For example, 2 identical doubly fed induction generator (DFIG) WTs may have different control algorithms. A DFIG WT can be operated in voltage-controlled mode or in power factor mode, for instance.

The grouping of the WTs can be performed based on other criteria, including line impedance, transformer and generator size, short-circuit capacity, protection relay setting, control set-points, and reactive compensation methods [2,12].

In this work, grouping is based on the same wind speed and the turbine locations. The typical wind farm is divided into 5 groups, as shown in Figure 4. As can be seen, each group has a different number of turbines. For example, group 1 has 15 turbines, whereas group 2 includes 7 turbines. In the MTR method, different wind

profiles are used for each WT group. The time series of the wind speed is subdivided into several sections and each subdivision is applied to a WT group.

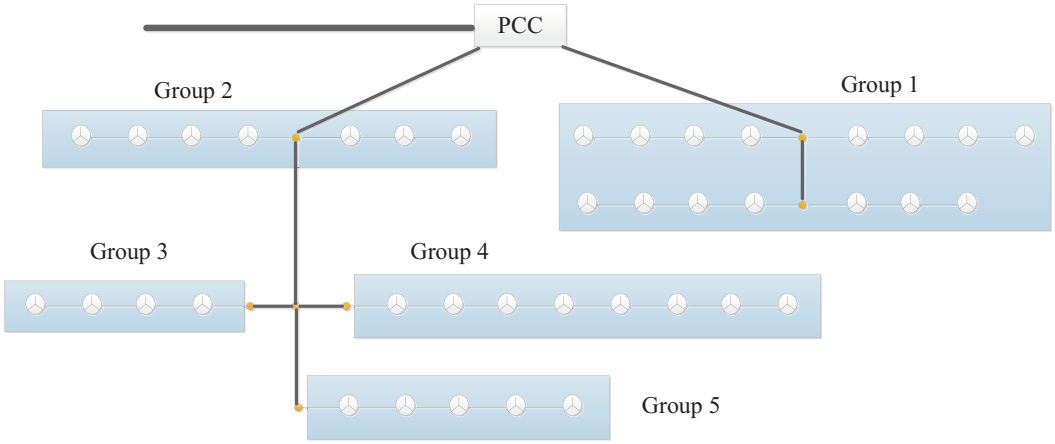

Figure 4. The wind turbine grouping in a typical wind farm.

4.1.3. Quasi-multiple turbine representation (QMTR)

QMTR considers the effect of different WTs on the network using STR [9]. MTR was introduced to overcome the drawbacks of the STR method, modeling several WTs with different wind input profiles. In MTR, the time series of the wind profile is subdivided into several sections and each subdivision is applied to a different group of the turbines, represented by a single WT.

In the QMTR method, the time series of the wind speed could be divided into 39 different files with different starting times. In [20], the time interval of 60 s between starting points has been considered. In this work also, the starting points have been randomly chosen from 0 to 2340 (39×60) s. Considering WTs as independent sources connected to a linear network, the mentioned wind subdivisions can be applied to the STR of the wind farm and the results can be superimposed from the network point of view [13]. In other words, this method applies the different wind profiles to the STR of the wind power plant and averages the results for the network quantities (i.e. the voltage, active power, and reactive power at the PCC).

Averaging in the QMTR method is performed based on the number of the WTs in the wind farm. In this paper, the averaging has been mostly done for 39 WTs to consider the effect of all the WTs of the wind farm. One advantage of the QMTR method is that the number of WTs can easily be changed, which corresponds to having a wind farm with a different number of WTs connected to a grid at the same short-circuit ratio (SCR) and grid X/R ratio. The SCR is defined by following equation:

$$SCR = \frac{S_k}{S_n}, \tag{23}$$

where S_k is the grid SCL at the PCC and S_n is the rated apparent power of the equivalent WTG.

4.1.4. Full turbine representation (FTR)

In this model, all turbines within the wind farm are modeled and the electrical connections between WTs within the farm are modeled accurately. The input wind profile of each turbine is considered to be different from the other turbine's input wind. The generated power and voltage of the system is available at every moment.

The FTR model of the wind farm is an excellent model for the wind farm. The accuracy of this method is known to be better if different types of WTs are utilized in the wind farm. The FTR method, however, has some disadvantages such as large computational load and long simulation time. It is not reasonable to simulate the entire wind farm by representing all individual turbines in the simulation [2].

4.2. Computational load of equivalents and full model

It is important to note that the time required to simulate a wind farm model is directly related to computational load. To simulate a typical wind farm with all WTs, the FTR method is used and its computational load is calculated by $\mathrm{C}_F = \mathrm{NC}_{wt}\mathrm{T}_F$, where N is the number of WTs in the wind farm, C_{wt} is the computational load to simulate one WT for 1 s, and T_F is the simulation time for the FTR. The computational load of each wind farm equivalent model is calculated by the following equations:

- STR computational load, C_s:

$$C_s = C_{wt}T_S, \tag{24}$$

  where T_S is simulation time for the STR.

- MTR computational load C_M:

$$C_M = MC_{wt}T_M, \tag{25}$$

  where M is the number of the WT groups in wind farm and T_M is the simulation time for the MTR.

- QMTR computational load C_Q:

$$C_Q = C_{wt}T_Q + C_{avr}, \tag{26}$$

  where T_Q is the simulation time for the QMTR and C_{avr} is the computational load required to average variables for the PCC.

In this research, the number of WTs is considered as 39 (N = 39). To equalize the computational loads of MTR and QMTR, the wind farm is divided into 5 groups (M = 5). Simulation times for STR, MTR, and FTR are equal to 600 s ($\mathrm{T}_F = \mathrm{T}_S = \mathrm{T}_M = 600$), but the simulation time of QMTR is equal to 2940 s ($\mathrm{T}_Q = 600 + 39 \times 60$). Assuming $\mathrm{C}_{ave} \cong \mathrm{C}_{wt}$ it can be concluded that $\mathrm{C}_F = 8\mathrm{C}_M = 8\mathrm{C}_Q = 39\mathrm{C}_S$.

5. Simulation structure and tools

VisSim software is used to implement the STR, MTR, QMTR, and FTR of the wind farm. Using VisSim, a modular simulation tool called RPM-Sim was developed to facilitate a low-cost application-specific study of the dynamics of the wind-solar-diesel hybrid power systems by Bialasiewicz and Muljadi [15]. The simple model of the FSWT, taken from RPM-Sim, is used to simulate the WTs in this research. VisSim is used to simulate other parts of the network such as the transformers, village load, transmission line, and infinite bus. The 2-dimensional turbulent wind is simulated by TurbSim [21]. The simulation procedure will be described in more detail in the following section.

5.1. Wind simulation using TurbSim

TurbSim is a stochastic, full-field, and turbulent-wind simulator used to provide simulated inflow turbulence environments, which consist of several important fluid dynamic features known to adversely affect turbine aeroelastic response and loading, such as wind shear and tower shadow effect [21]. In this paper, TurbSim is used to simulate a 6×6 point grid wind with turbulent intensity of 'A' and a mean speed of 11.5 m/s (at 60 m hub height). It should be noted that there are 2 ways to determine wind turbulence intensity in TurbSim. The turbulence intensity can be determined either in percent or by one of the standard IEC classifications of turbulence. The IEC standard classifications are presented in 3 classes: A, B, and C. A has the highest turbulence.

For this research, a 2940 s wind profile is produced by TurbSim. A time interval of 60 s between starting points was considered. For example, for the first turbine the range of the wind input is from 0 to 600, and for the second turbine, the input time interval is from 60 to 660. Figure 5 shows the wind input of the first turbine in the FTR. Figure 6 shows the wind speed at hub height for 2940 s. As can be seen in Figure 6, the wind speed range varies from 5 to 18 m/s.

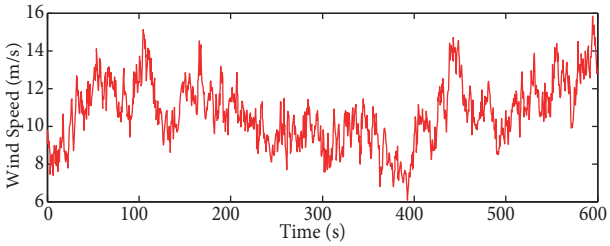

Figure 5. Input wind speed to the first wind turbine.

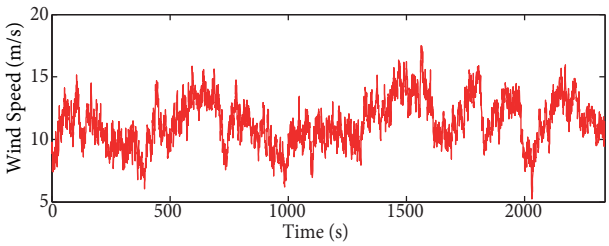

Figure 6. Total input wind speed for wind farm.

5.2. Wind farm and power system simulation using VisSim

There are various software programs that simulate WTs and wind farms. For example, PSCAD, MATLAB, PSS/E, and FAST software can be used to simulate a wind farm using a STR model [6,7,9,10]. These WT dynamic models are complicated because the software considers many degrees of freedom for mechanical parts and other parts like the generator and grid. In FTR, however, it can create a huge computational load on the simulator, since all of the WTs in the wind farm should be simulated.

This research basically focuses on the wind farm equivalent models, not the WT model. Considering this subject, a simpler WT model with few degrees of freedom for mechanical and electrical parts may be used to compare different wind farm models. In this regard, the RPM-Sim wind turbine model, developed in a VisSim environment, is used in this research. Other software programs, e.g. FAST, consider many degrees of freedom for mechanical parts, which is not necessary for this research. Moreover, VisSim has a special ability to run heavy simulations. The modeling in VisSim is performed based on d-q axis components. The SCIG simple model of RPM-Sim is used to model the wind farm. The view of VisSim blocks, shown in Figures 7 and 8, depicts the blocks of the WT model taken from RPM-Sim.

In VisSim software, each FSWT is simulated with 4 blocks. The WT rotor is simulated in the first block and its input is the wind speed. The most important part of this block is related to the nonlinear relation between TSR and the power coefficient, C_p, which is encapsulated in the map block. The second block is the gearbox model, in which the gear ratio is declared and the high-velocity torque is calculated, appended with a negative sign for future calculations [16]. The third block includes the induction generator model.

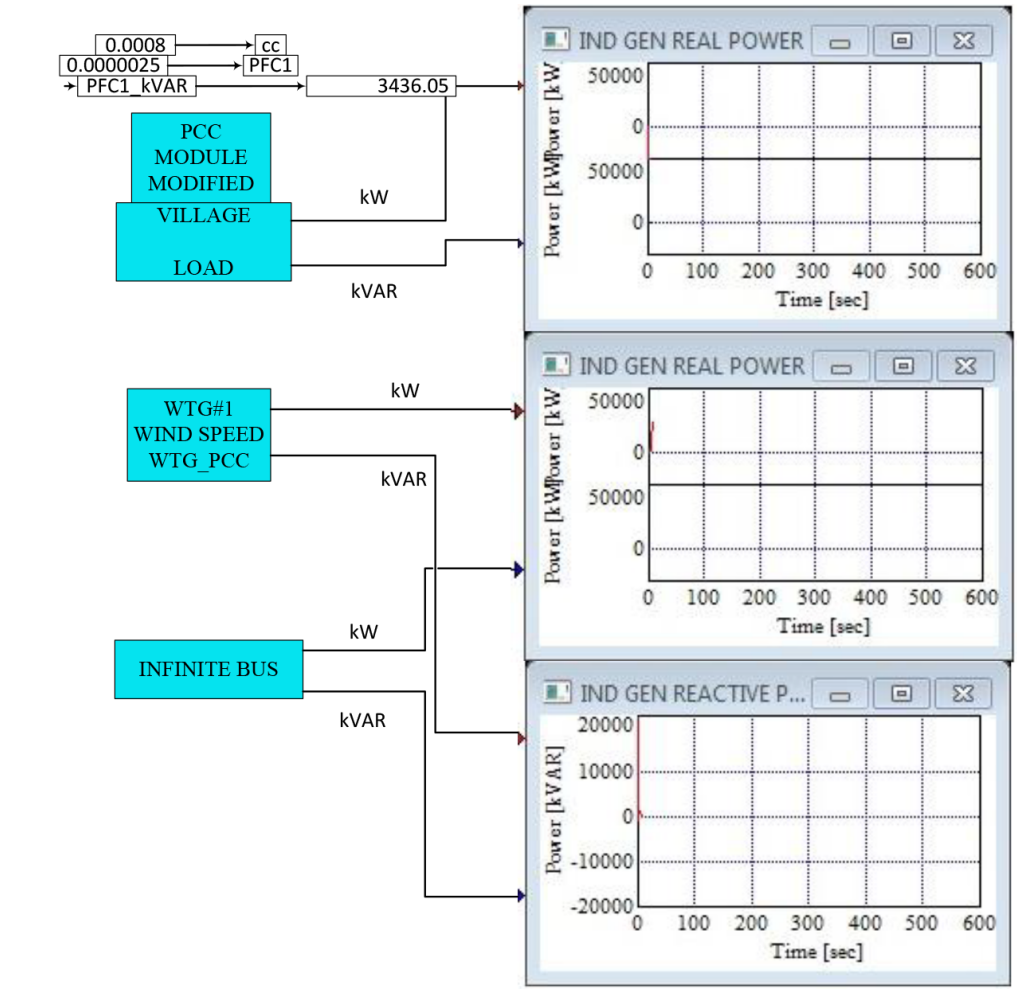

Figure 7. A view of the whole power system simulation in VisSim.

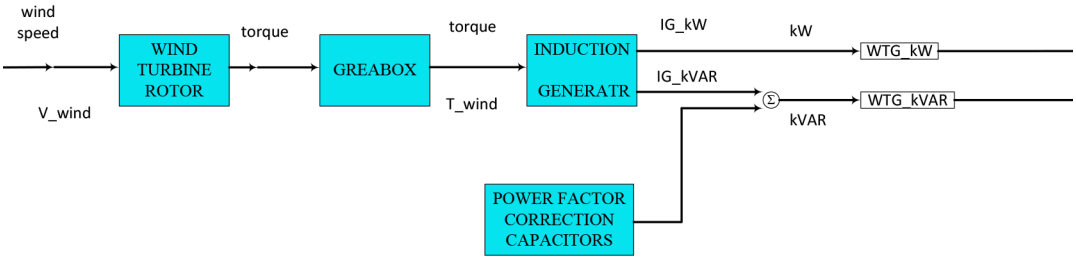

Figure 8. The wind turbine model in RPM-Sim.

Finally, the fourth block is the power factor correction capacitor that models capacitance and line impedance in the output of the WT. In this simulation, the reactive power has 2 components: a component absorbed by the induction generator and a component contributed by the PFC capacitor block [16]. The WT parameters used in VisSim are given in Table 1.

To implement the FTR, the RPM-Sim turbine model should be modified. The fourth block of the WT model is changed to model the daisy-chain connections of the WT. The summation of the daisy-chains' generated currents is calculated in the PCC WT-GEN block. Other parts of the power system are modeled using

an impedance model. For example, a reactance (X_S) is used to model the transformer and the transmission line is modeled with an impedance ($Z_{line} = R_{line} + JX_{line}$). The power system connection is considered as an infinite bus in this research.

Table 1. Comparison of active power change between models.

WF model	Minimum power (kW)	Maximum power (kW)	Change (%)
STR	5437	38,985	86
MTR	16,513	31,802	39.2
QMTR	25,299	29,895	11.8
FTR	25,475	29,930	11.4

5.3. Implementation of the IEEE flickermeter using VisSim

The IEEE flickermeter is applied in the VisSim environment. The flickermeter is made of 6 transfer functions that are shown in Figure 9. Block A prepares the per unit voltage and performs quadratic demodulation of the voltage signal. Block B eliminates the DC voltage component and high-frequency fluctuations found at the output of the quadratic demodulator. The frequency response of the human eye to the voltage fluctuations of an incandescent lamp supplied by a variable sinusoidal voltage is modeled by block C. Block D models the nonlinear perception of the flicker in the eye–brain chain. Block E presents a low-pass filter that models the behavior of the flicker memorization in the brain. Instantaneous flicker cannot be a suitable criterion for system flicker emission assessment. Generally, a short-term index (P_{st}) and long-term index (P_{lt}) are used as system flicker criteria. Block F calculates the P_{st} based on the IEC 61000-4-15 standard [22].

$$P_{st} = \sqrt{0.0314P_{0.1} + 0.0525P_{1s} + 0.0657_{3s} + 0.28P_{10s} + 0.08P_{50s}} \tag{27}$$

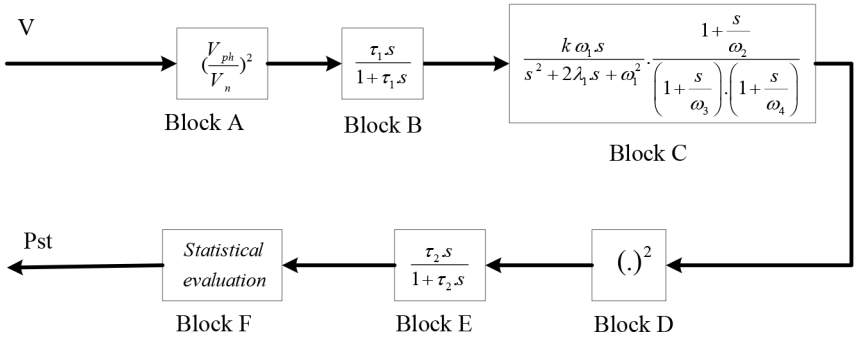

Figure 9. The block diagram of the flickermeter [24].

6. Simulation results

The impact of the wind velocity fluctuations and tower shadow on the system voltage and the active and reactive powers at the PCC with 4 different wind power plant representations (i.e. STR, MTR, QMTR, and FTR) are studied in this paper.

Figure 10 shows the variation of the system voltage for all 4 representations taken at the PCC bus. The voltage variation of STR changes from 0.975 pu to 1.01 pu. As a result, large fluctuations are observed in the STR. As expected, the voltage variation in MTR is less and changes from 0.9874 pu to 1.0056 pu. However, the QMTR result is very interesting because it is very close to that of FTR. The QMTR voltage variation is from 0.9949 pu to 1.0007 pu, while the FTR voltage variation changes from 0.9939 pu to 1.0007 pu.

Figure 11 shows the variation of the system active and reactive powers for all 4 representations taken at the PCC. As can be seen, the wind fluctuations cause variations in the powers. In STR, the variations reflect the power and voltage fluctuation of a single turbine [9], whereas for MTR, QMTR, and FTR, the power and voltage fluctuations are the collective behavior of the WTs fed by different wind profiles as described in section 4. The ranges of the active and reactive power changes are presented in Tables 1 and 2.

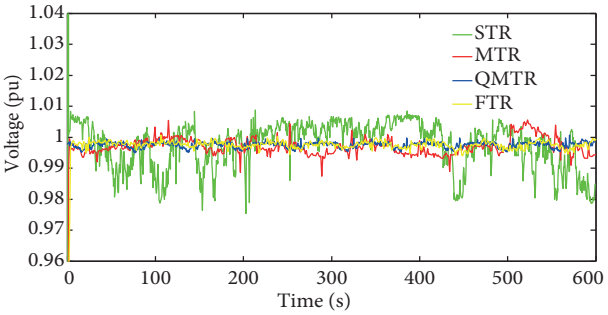

Figure 10. The voltage at PCC for STR (thinner), MTR (thin), QMTR (thick), and FTR (thicker).

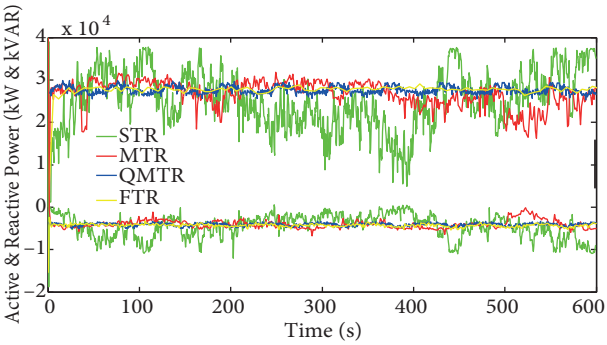

Figure 11. The active (top) and reactive (down) powers at PCC, STR (thinner), MTR (thin), QMTR (thick), and FTR (thicker).

Table 2. Comparison of reactive power change between models.

WF model	Minimum power (kW)	Maximum power (kW)	Change (%)
STR	–1204	504	62.7
MTR	–6745	–95	33.2
QMTR	–5079	–3323	8.8
FTR	–5406	–3260	10.7

In this work, 2 methods have been presented to study and compare the equivalent models. The first method studies the comparison of the equivalent models at any moment in time. To achieve this, the differences of the PCC parameters between equivalent models and the FTR are calculated at any moment in time. In Figure 12, voltage deviation in the equivalent models compared with the FTR is presented. The STR voltage deviation is much more than that of the other models and QMTR has the lowest voltage deviation. The active and reactive power deviations are shown in Figures 13 and 14, respectively. In both of them, QMTR has the lowest deviation. For example, maximum active power deviation in QMTR is equal to 2642 kW while in MTR it is equal to 11,942 kW and in STR it is equal to 20,511 kW.

The second method presents percent change of the equivalent models. The difference between the maximum and minimum values of these parameters divided into the nominal can be considered as a criterion for measuring fluctuations. This criterion is called the percent change.

As can be seen in Figure 10, the PCC bus voltage percent changes are different in various models. The percent change in STR is equal to 3.46%, in MTR it is equal to 1.82%, in QMTR it is equal to 0.58%, and in FTR it is equal to 0.68%. STR shows the closest percent change to that of FTR. Therefore, QMTR is the best equivalent model. For a detailed study, other signals of the equivalent models such as the active and reactive powers of the PCC bus should be compared. In Figure 11, the percent changes of the active and reactive powers are given as in Tables 1 and 2. Comparing the given values, it can be calculated that QMTR, MTR, and STR are the closest methods to FTR, respectively.

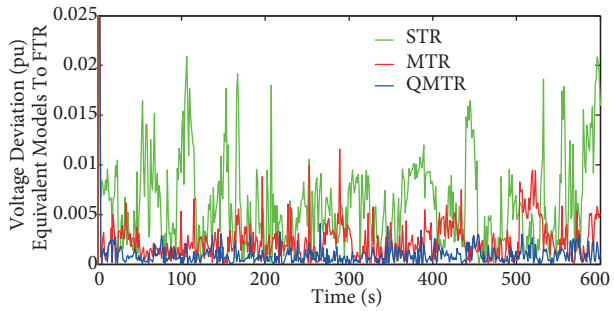

Figure 12. Equivalent models' voltage deviation compared to FTR.

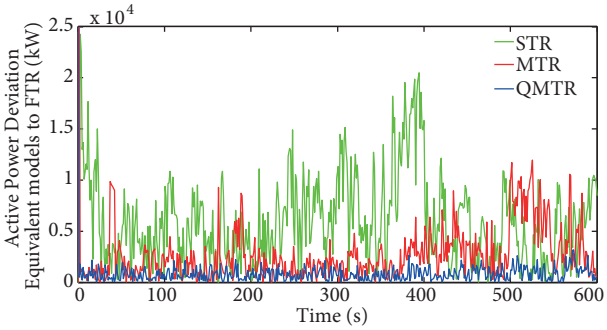

Figure 13. Equivalent models' active power deviation compared to FTR.

Figure 15 shows the flicker level at the PCC bus in different wind farm models. In STR, the flicker level is more than that of any other wind farm model. In MTR, the flicker fluctuations are decreased compared with the STR model. QMTR has the closest flicker level to FTR. Flicker short-term index (P_{st}) is shown in Table 3. It should be mentioned that the QMTR P_{st} value is less than the FTR value because in QMTR, the averaging method is performed and interactions between WTs are not considered, but even so, the QMTR P_{st} value is the closest value to the FTR value between different wind farm models. Due to P_{st} values, the importance of wind farm modeling is apparent because, according to the IEC standard [23], this wind farm cannot be connected to the utility grid if STR is selected for modeling but connection to the utility grid is permitted if FTR is used to model the wind farm.

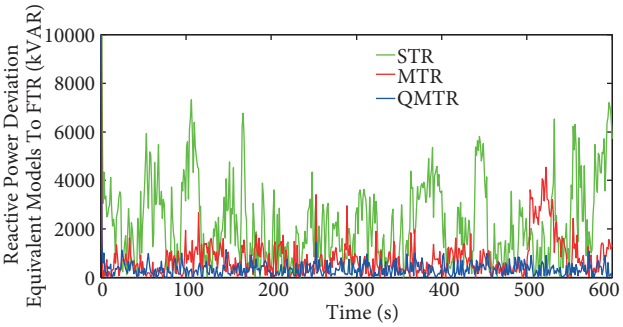

Figure 14. Equivalent models reactive power deviation compared to FTR.

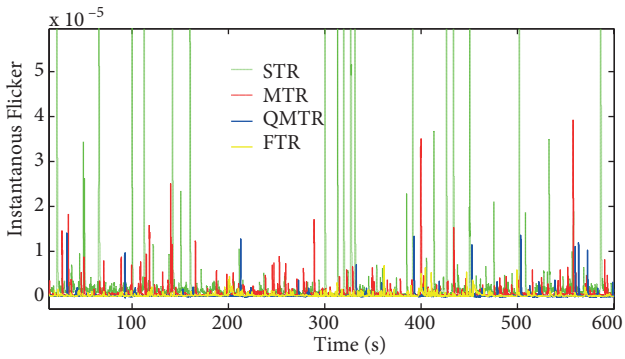

Figure 15. Instantaneous flicker in PCC bus.

Table 3. Flicker short-term index in different wind farm models.

WF model	STR	MTR	QMTR	FTR
P_{st}	1.12	0.65	0.3875	0.4312

7. Conclusion

In this research, a typical wind farm with 39 SCIG WTs was modeled using 4 different modeling methods (i.e. STR, MTR, QMTR, and FTR). The models include 3 equivalent models and a full model. The full model of the wind farms is utilized as an appropriate criterion to measure the accuracy of the equivalent models. The full modeling of a large wind farm is very difficult and sometimes impossible. A medium-sized wind farm is modeled in this research.

In this paper, the computational load and accuracy of the equivalent models (i.e. STR, MTR, and QMTR) were compared with the full model of the wind farm. To compare the accuracy of MTR and QMTR, the computational load of both methods were considered the same, choosing an appropriate number of WTs in the MTR method. The accuracy of the models was compared investigating 4 network parameters at the PCC. Voltage fluctuation is one of these parameters in this comparison that is important in power quality studies. The STR method shows the highest voltage and flicker variations compared to FTR, and so it has the lowest accuracy. QMTR shows the best accuracy in the voltage and flicker comparison, since it has the least deviation from FTR. The accuracy of MTR is higher than that of STR and lower than that of QMTR.

The other important parameters in the comparison of the models are active and reactive powers. The correct prediction of the active power is very important in power system planning. The active and reactive power fluctuations are highest for STR, medium for MTR, and the lowest for QMTR. According to the results, QMTR shows the closest result to FTR. Therefore, it can be concluded that QMTR presents the best equivalent model for a SCIG-based wind farm.

Nomenclature

ρ, V_{wind}	air density and wind velocity
$R_{bld}, Gear_r$	rotor radius and gear ratio
ω_r	induction machine angular velocity
θ	pitch angle of the rotor blades
rpm	induction machine speed
λ, C_P	tip speed ratio and power coefficient
P_{wind}	extracted power from the wind
H	equivalent constant inertia of the rotating mass
S	slip of the squirrel-cage induction generator
T_e	electromagnetic torque of the squirrel-cage induction generator
v_{ds}, v_{qs}	stator voltages in the d and q axes
v'_{dr}, v'_{qr}	rotor voltages in the d and q axes
Ψ_{ds}, Ψ_{qs}	stator flux linkage in the d and q axes
$\Psi\prime_{dr}, \Psi\prime_{qr}$	rotor flux linkage in the d and q axes
ω_b	base synchronous speed
ω_s	synchronous speed
$r_s + jx_{ls}$	stator impedance
$r'_r + jx'_{lr}$	rotor impedance
X_m	magnetizing reactance
L_{ss}, L_{rr}	stator and rotor self-inductance
L_m	inductance between stator and rotor windings

References

[1] Hand M, Blair N, Bolinger M, Wiser R, O'Connell R, Hern T, Miller B. Power system modeling of 20 wind-generated electricity by 2030. In: IEEE Power Engineering Society General Meeting; July 2008; Pittsburgh, PA, USA. New York, NY, USA: IEEE. pp. 1-8.

[2] Muljadi E, Parsons B. Comparing single and multiple turbine representations in a wind farm simulation. In: European Wind Energy Conference; February 2006; Athens, Greece. Golden, CO, USA: NREL. pp. 1-10.

[3] Ali M, Ilie IS, Milanovic JV, Chicco G. Wind farm model aggregation using probabilistic clustering. IEEE T Power Deliver 2013; 28: 309-316.

[4] Han X, Qu Y, Wang P, Yang J. Four-dimensional wind speed model for adequacy assessment of power systems with wind farms. IEEE T Power Syst 2013; 28: 2978-2985.

[5] Zubia I, Ostolaza X, Susperregui A, Tapia G. Complete wind farm electromagnetic transient modelling for grid integration studies. Energ Convers Manage 2009; 50: 600-610.

[6] Qiao W, Harley RG, Venayagamoorthy GK. Dynamic modeling of wind farms with fixed speed wind turbine generators. In: IEEE Power Engineering Society General Meeting; 24–28 June 2007; Tampa, FL, USA. New York, NY, USA: IEEE. pp. 1-8.

[7] Fernandez L, Garcia C, Saenz J, Jurado F. Equivalent models of wind farms by using aggregated wind turbines and equivalent winds. Energ Convers Manage 2009; 50: 691-704.

[8] Meng ZJ, Xue F. An investigation of the equivalent wind method for the aggregation of DFIG wind turbines. In: Power and Energy Engineering Conference Asia-Pacific; March 2010; Chengdu, China. New York, NY, USA: IEEE. pp. 1-6.

[9] Fadaeinedjad R, Moschopoulos G, Moallem M. A new wind power plant simulation method to study power quality. In: IEEE Canadian Conference on Electrical and Computer Engineering; April 2007; Vancouver, Canada. New York, NY, USA: IEEE. pp. 1433-1436.

[10] Feltes JW, Fernandes BS, Keung PK. Case studies of wind park modeling. In: IEEE Power and Energy Society General Meeting; July 2011; San Diego, CA, USA. New York, NY, USA: IEEE. pp. 1-7.

[11] Kanellos FD, Kabouris J. Wind farms modeling for short-circuit level calculations in large power systems. IEEE T Power Deliver 2009; 24: 1687-1695.

[12] Muljadi E, Pasupulati S, Ellis A, Kosterov D. Method of equivalencing for a large wind power plant with multiple turbine representation. In: IEEE Power and Energy Society General Meeting; July 2008; Pittsburgh, PA, USA. New York, NY, USA: IEEE. pp. 1-9.

[13] Fadaeinedjad R, Moallem M, Moschopoulos G, Bassan S. Flicker contribution of a wind power plant with single and multiple turbine representations. In: IEEE Electrical Power Conference; October 2007; Montreal, Canada. New York, NY, USA: IEEE. pp. 74-79.

[14] Borrello M, Corbeil A, Kolk R. VisSim User's Guide Version 8.0. Westford, MA, USA: Visual Solutions, 2010.

[15] Bialasiewicz JT, Muljadi E. Analysis of renewable-energy systems using rpm-sim simulator. IEEE T Ind Electron 2006; 53: 1137-1143.

[16] Bialasiewicz J, Muljadi E, Drouilhet S, Nix G. Modular simulation of a hybrid power system with diesel and wind turbine generation. In: Proceedings of the American Control Conference; June 1998; Philadelphia, PA, USA. New York, NY, USA: IEEE. pp. 1705-1709.

[17] Li H, Chen Z, Han L. Comparison and evaluation of induction generator models in wind turbine systems for transient stability of power system. In: International Conference on Power System Technology; October 2006; Chongqing, China. New York, NY, USA: IEEE. pp. 22-26.

[18] Iov F, Hansen AD, Sorensen P, Blaabjerg F. Wind turbine blockset in MATLAB/Simulink. Aalborg, Denmark: Aalborg University, 2004.

[19] Muljadi E, Butterfield C, Ellis A, Mechenbier J, Hochheimer J, Young R, Miller N, Delmerico R, Zavadil R, Smith J. Equivalencing the collector system of a large wind power plant. In: IEEE Power Engineering Society General Meeting; June 2006; Montreal, Canada. New York, NY, USA: IEEE.

[20] Muljadi E, Butterfield C, Chacon J, Romanowitz H. Power quality aspects in a wind power plant. In: IEEE Power Engineering Society General Meeting; June 2006; Montreal, Canada. New York, NY, USA: IEEE.

[21] Jonkman B. TurbSim user's guide. NREL TP-500-46198. Golden, CO, USA: NREL, 2009.

[22] IEC. IEC 61000-4-15. Flickermeter-Functional and Design Specifications. IEC Standard, Ed 1.1. Geneva, Switzerland: IEC, 2003.

[23] IEC. IEC 61400-21. Wind Turbine Generator Systems - Part 21: Measurement and Assessment of Power Quality Characteristics of Grid Connected Wind Turbines. IEC Standard. Geneva, Switzerland: IEC, 2001.

[24] Bertola A, Lazaroiu GC, Roscia M, Zaninelli D. A MATLAB-Simulink flickermeter model for power quality studies. In: 11th International Conference on Harmonics and Quality of Power; September 2004; Lake Placid, CA, USA. New York, NY, USA: IEEE. pp. 734-438.